Separation Science and Technology
Publication details, including instructions for authors and subscription information:
http://www.informaworld.com/smpp/title~content=t713708471

The Instrument Spreading Correction in GPC. II. The General Shape Function Using the Fourier Transform Method with a Nonlinear Calibration Curve

Edward M. Rosen[a]; Theodore Provder[ab]
[a] MONSANTO COMPANY, ST. LOUIS, MISSOURI [b] SCM Corporation, Glidden-Durkee Division, Dwight P. Joyce Research Center, Strongsville, Ohio

To cite this Article Rosen, Edward M. and Provder, Theodore(1970) 'The Instrument Spreading Correction in GPC. II. The General Shape Function Using the Fourier Transform Method with a Nonlinear Calibration Curve', Separation Science and Technology, 5: 4, 485 — 521
To link to this Article: DOI: 10.1080/00372367008068443
URL: http://dx.doi.org/10.1080/00372367008068443

SEPARATION SCIENCE, 5(4), pp. 485–521, August, 1970

The Instrument Spreading Correction in GPC. II. The General Shape Function Using the Fourier Transform Method with a Nonlinear Calibration Curve*

EDWARD M. ROSEN and THEODORE PROVDER†
MONSANTO COMPANY
ST. LOUIS, MISSOURI 63166

Summary

The instrument spreading function suggested in Part I of this series is investigated for use with the Fourier transform method for generating corrected elution volume chromatograms. The instrument spreading parameters are obtained using linear theory on narrow molecular weight distribution standards, as indicated in Part I. The corrected chromatogram is then combined with a nonlinear molecular weight calibration curve which was fit with a function suggested by Yau and Malone to generate true values of the number- and weight-average molecular weights.

The instrument spreading function is shown to qualitatively and quantitatively describe the dispersion, skewing, and flattening effects ordinarily found in GPC chromatograms due to imperfect resolution by the GPC columns. The Yau-Malone function is shown to be a very useful function for fitting nonlinear molecular weight vs elution volume calibration data. Although the Fourier transform method is shown to work well with analytically generated data, it is shown that a number of numerical problems must be overcome before it can quantitatively produce corrected elution volume chromatograms. Some of these numerical problems are discussed.

* Presented at the ACS Symposium on Gel Permeation Chromatography, sponsored by the Division of Petroleum Chemistry at the 159th National Meeting of the American Chemical Society, Houston, Texas, February, 1970.

† Author to whom all correspondence should be addressed at: SCM Corporation, Glidden-Durkee Division, Dwight P. Joyce Research Center, 16651 Sprague Road, Strongsville, Ohio 44136.

1. INTRODUCTION

In the first paper of this series (*1*) [denoted as (I.) throughout the present paper], a general instrument spreading function was suggested which, together with a linear molecular weight calibration curve, was used to correct the infinite resolution gel permeation chromatography (GPC) number- and weight-average molecular weights and intrinsic viscosities, denoted respectively by $\bar{M}_n(\infty)$, $\bar{M}_w(\infty)$, and $[\eta](\infty)$, to their true values, denoted respectively by $\bar{M}_n(t)$, $\bar{M}_w(t)$ and $[\eta](t)$. In addition, it was shown that the hydrodynamic volume concept could be used to evaluate a reasonable approximation to the corrected differential molecular weight distribution (DMWD) curves.

This approach had three major limitations. (a) The $\log_{10} M$ vs elution volume calibration curve had to be linear over the elution volume range of interest. (b) The instrument spreading correction factors were assumed to be constant over the elution volume range of interest. (c) The corrected elution volume chromatogram could not be calculated directly.

In order to overcome the first difficulty, use was made of a nonlinear calibration curve, the functional form of which was suggested by Yau and Malone (*2*). To circumvent the second and third limitations, use was made of the Fourier transform method (*3*, *4*).

2. THE INSTRUMENT SPREADING FUNCTION

Tung (*3*) has shown that the normalized (i.e., area under the curve is unity) observed GPC chromatogram $F(v)$ at elution volume v is related to the instrument spreading function $G(v - y)$ and the normalized corrected chromatogram $W(v)$ by means of the equation

$$F(v) = \int_{-\infty}^{\infty} G(v - y)W(y)\, dy \tag{1}$$

where $F(v)$ is known, $G(v - y)$ is postulated, and $W(y)$ is to be evaluated. Physically, $G(v - y)$ can be thought of as the distribution function of elution volume about an elution volume y describing the shape of the chromatogram resulting from an ideal monodisperse species passing through a set of GPC columns, and $W(y)$ as the weighting factor for the species such that Eq. (1) is satisfied. Whatever form is chosen for $G(v - y)$, it should be capable of describing the behavior of the observed chromatogram of a nearly monodisperse standard.

As indicated in (I.), the instrument spreading function chosen has been widely used in the statistical literature (*5*, *6*) to describe perturbed Gaussian density functions and recently has been used to describe

chromatogram shapes in gas–liquid chromatography (7). The instrument spreading function is given by

$$G(x) = \phi(x)\left[1 + \sum_{n=3}^{\infty} (A_n/n!)H_n(x)\right] \tag{2}$$

where

$$\phi(x) = (1/2\pi)^{1/2} \exp(-x^2/2) \tag{3}$$

and

$$x = (v - y)/\sqrt{\mu_2} \tag{4}$$

$H_n(x)$ are the Hermite polynomials defined in Table 1 and μ_2 is the

TABLE 1

Properties of Hermite Polynomials

Hermite Polynomials

$$H_0(x) = 1$$
$$H_1(x) = x$$
$$H_2(x) = x^2 - 1$$
$$H_3(x) = x^3 - 3x$$
$$H_4(x) = x^4 - 6x^2 + 3$$

Generating Function

$$\sum_{m=0}^{\infty} \frac{H_m(x)}{m!} t^m = \exp[t^2/2 + tx]$$

Orthonormality Relationship

$$(1/2\pi)^{1/2} \int_{-\infty}^{\infty} H_n(x)H_m(x) \exp(-x^2/2)\, dx = \begin{cases} n! & n = m \\ 0 & n \neq m \end{cases}$$

second moment of the instrument spreading function about an elution volume y. When $A_n = 0$ for $n \geq 5$, Eq. (2) becomes the Gram-Charlier (A) series which shall be used throughout this paper and is given by

$$G(v - y) = (1/2\pi\mu_2)^{1/2} \exp[-(v - y)^2/2\mu_2] \times \{1 + (A_3/3!)H_3[(v - y)/\sqrt{\mu_2}] + (A_4/4!)H_4[(v - y)/\sqrt{\mu_2}]\} \tag{5}$$

where A_3 and A_4 are skewing and flatness parameters defined by the equations

$$A_3 = \mu_3/\mu_2^{3/2} = \sqrt{\beta_1} \tag{6}$$
$$A_4 = \mu_4/\mu_2^2 - 3 = \beta_2 - 3 \tag{7}$$

The parameters μ_2, μ_3, and μ_4 are the second, third, and fourth moments of $G(v - y)$ about elution volume y. In general,

$$\mu_n = \int_{-\infty}^{\infty} (v - y)^n G(v - y)\, d(v - y) \qquad n = 2, 3, 4 \qquad (8)$$

Since the instrument spreading parameters μ_n cannot be measured directly, they will be determined by an indirect procedure. Barton and Dennis (*8*) examined Eq. (5) for regions in which it remained positive definite and unimodal. Their results are shown in Fig. 1 in terms of the parameters β_1 and β_2 defined by Eqs. (6) and (7). The corresponding regions for the Edgeworth series (Eq. 2 with $A_6 = 10A_3^2$ and $A_n = 0$ for $n \geq 7$) used in (I.) are also shown. Figure 1 shall be referred to in the discussion of the determination of the instrument spreading parameters in Section 6.

A number of relationships between the moments of $F(v)$ and the moments of $W(y)$ can be derived directly from Eqs. (1) and (2) by using the properties of the Hermite polynomials. These relationships together with the notations used are summarized in Table 2.

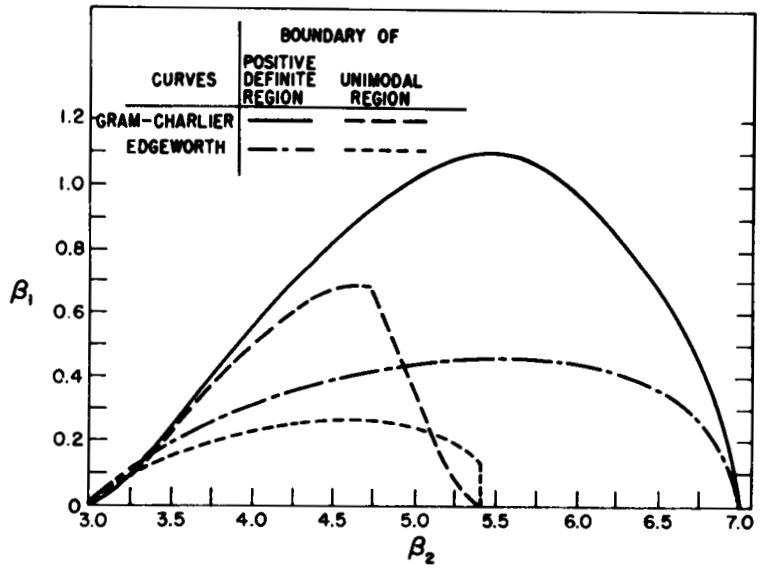

FIG. 1. Unimodal and positive definite regions in the β_1-β_2 plane for Gram-Charlier and Edgeworth Curves.

TABLE 2

Nomenclature and Relationships Among the Moments of the Raw and Corrected Chromatograms and the Instrument Spreading Function

Nomenclature			
Parameter	Raw chromatogram $F(v)$ (moments about μ)	Instrument spreading function $G(v\text{-}y)$ (moments about y)	Corrected chromatogram $W(v)$ (moments about μ)
Unnormalized area	A	1	A
Normalized area	1	1	1
Mean	μ	0	μ
Second moment	m_2	μ_2	m_2^*
Third moment	m_3	μ_3	m_3^*
Fourth moment	m_4	μ_4	m_4^*

Moment	Relation
Zero	Area of unnormalized $W(v)$ = Area of unnormalized $F(v)$
First	Mean of $W(v)$ = Mean of $F(v)$
Second	$m_2^* = m_2 - \mu_2$
Third	$m_3^* = m_3 - \mu_3$
Fourth	$m_4^* = m_4 - 6\mu_2 m_2 + 6\mu_2^2 - \mu_4$

To illustrate the general method used to derive these relationships, consider the third moment calculations. The third moment about zero elution volume is given by

$$\langle v^3 \rangle = \int_{-\infty}^{\infty} v^3 F(v)\, dv = \int_{-\infty}^{\infty} \int_{-\infty}^{\infty} v^3 G(v - y) W(y)\, dy\, dv \tag{9}$$

Substituting Eqs. (2), (3), and (4) into (9) and reversing the order of integration yields

$$\langle v^3 \rangle = \int_{-\infty}^{\infty} W(y) \int_{-\infty}^{\infty} \phi(x)[H_0(x) + (A_3/3!)H_3(x) + (A_4/4!)H_4(x)] \cdot [\sqrt{\mu_2}x + y]^3\, dx\, dy \tag{10}$$

Expanding and integrating term by term yields

$$\langle v^3 \rangle = \int_{-\infty}^{\infty} W(y)[A_3\mu_2^{3/2} + 3\mu_2 y + y^3]\, dy \tag{11}$$

Then

$$\langle v^3 \rangle = \langle y^3 \rangle + A_3\mu_2^{3/2} + 3\mu_2\mu \tag{12}$$

Expressing Eq. (12) in terms of moments about the mean results in the following relation

$$m_3^* = m_3 - \mu_3 \tag{13}$$

3. THE FOURIER TRANSFORM METHOD

Equation (1) is an integral equation of the convolution type and classically has been solved by means of Fourier transforms. This transformation is performed because the relationship can be reduced to a simple algebraic expression in the transformed k-space. Following Tung (*3*), the Fourier transform of both sides of Eq. (1) yields the relation

$$W(k) = (1/2\pi)^{1/2}[F(k)/G(k)] \tag{14}$$

where

$$F(k) = (1/2\pi)^{1/2} \int_{-\infty}^{\infty} F(v) \exp(ikv)\, dv \tag{15}$$

$$G(k) = (1/2\pi)^{1/2} \int_{-\infty}^{\infty} G(v - y) \exp[ik(v - y)]\, d(v - y) \tag{16}$$

$$W(k) = (1/2\pi)^{1/2} \int_{-\infty}^{\infty} W(v) \exp(ikv)\, dv \tag{17}$$

and

$$F(k) = F_r(k) + iF_i(k) \tag{18}$$

$$G(k) = G_r(k) + iG_i(k) \tag{19}$$

$$W(k) = W_r(k) + iW_i(k) \tag{20}$$

Use of Eqs. (18), (19), and (20) in Eq. (14) leads to the following relations for $W_r(k)$ and $W_i(k)$

$$W_r(k) = \frac{F_r(k)G_r(k) + F_i(k)G_i(k)}{\sqrt{2\pi}\,[G_r^2(k) + G_i^2(k)]} \tag{21}$$

$$W_i(k) = \frac{F_i(k)G_r(k) - F_r(k)G_i(k)}{\sqrt{2\pi}\,[G_r^2(k) + G_i^2(k)]} \tag{22}$$

Once $W(k)$ is determined, $W(v)$ can be obtained from

$$W(v) = (1/2\pi)^{1/2} \int_{-\infty}^{\infty} W(k) \exp(-ikv)\, dv \tag{23}$$

Upon noting that $W_r(k)$ and $W_i(k)$ are even and odd functions, respectively, in k-space, $W(v)$ can be expressed in terms of $W_r(k)$ and $W_i(k)$ by the equation

$$W(v) = (1/2\pi)^{1/2} \int_{-\infty}^{\infty} [W_r(k) \cos(kv) + W_i(k) \sin(kv)]\, dk \quad (24)$$

The operational procedure used for the determination of $W(v)$ consists of the following steps. First, $F_r(k)$ and $F_i(k)$ are numerically evaluated from the normalized observed chromatogram $F(v)$.

$$F_r(k) = (1/2\pi)^{1/2} \int_{-\infty}^{\infty} F(v) \cos(kv)\, dv \quad (25)$$

$$F_i(k) = (1/2\pi)^{1/2} \int_{-\infty}^{\infty} F(v) \sin(kv)\, dv \quad (26)$$

Using the generating function of Table 1 and Eqs. (5), (6), and (7) in Eqs. (16) and (19), analytical expressions are obtained for $G_r(k)$ and $G_i(k)$.

$$G_r(k) = (1/2\pi)^{1/2} \exp(-k^2\mu_2/2)[1 + (k^4/24)(\mu_4 - 3\mu_2^2)] \quad (27)$$

$$G_i(k) = (1/2\pi)^{1/2} \exp(-k^2\mu_2/2)[-k^3\mu_3/6] \quad (28)$$

Upon knowing or assuming values for μ_2, μ_3, and μ_4, $G_r(k)$ and $G_i(k)$ are evaluated and then $W_r(k)$ and $W_i(k)$ are obtained from Eqs. (21) and (22). Finally, $W(v)$ is evaluated from Eq. (24).

Although the parameters μ_2, μ_3, and μ_4 are assumed to be constants or slowly varying functions of the elution volume v during the integrations, in general they shall be considered to be strong functions of the elution volume v in the evaluation of $W(v)$. In general, $G(k)$ and $W(k)$ then will both be functions of v. This inconsistency will remain a limitation of the method, particularly when μ_2, μ_3, and μ_4 are no longer slowly varying functions of v. Note, however, regardless of the nature of $G(k)$, $F(k)$ needs to be evaluated only once because it is only a function of the observed chromatogram.

4. NUMERICAL PROCEDURES

The evaluation of the integrals in Eqs. (25) and (26) have been the subject of considerable numerical investigations (*9*, *10*). Tung (*3*) used the discrete Fourier transform (DFT), which considers the integrals as infinite sums.* The fast Fourier transform (FFT) is an efficient method for the evaluation of the DFT when the number of data points tends to be very large. However, for GPC data the sampling interval is not excessively small nor is the range of elution volumes very large. Hence, the integral form can be used without excessive computational

* Examination of the Fortran computer program supplied by Dr. Tung indicated the use of the DFT.

work. In order to evaluate Eqs. (25) and (26), the range of integration must be transformed to some convenient point about the center of the chromatogram, v_0, which is an even multiple of the increment size used in k-space. Upon letting

$$z = v - v_0 \tag{29}$$

Eqs. (25) and (26) become

$$F_r(k) = \cos(kv_0)F_1(k) - \sin(kv_0)F_2(k) \tag{30}$$

and

$$F_i(k) = \cos(kv_0)F_2(k) + \sin(kv_0)F_1(k) \tag{31}$$

where

$$F_1(k) = (1/2\pi)^{1/2} \int_{-\infty}^{\infty} F(z) \cos(kz)\, dz \tag{32}$$

and

$$F_2(k) = (1/2\pi)^{1/2} \int_{-\infty}^{\infty} F(z) \sin(kz) \tag{33}$$

Under this transformation Eq. (24) becomes

$$W(v) = (1/2\pi)^{1/2} \int_{-\infty}^{\infty} [W_1(k) \cos(kz) + W_2(k) \sin(kz)]\, dk \tag{34}$$

where

$$W_1(k) = \frac{F_1(k)G_r(k) + F_2(k)G_i(k)}{\sqrt{2\pi}\,[G_r^2(k) + G_i^2(k)]} \tag{35}$$

$$W_2(k) = \frac{F_2(k)G_r(k) - F_1(k)G_i(k)}{\sqrt{2\pi}\,[G_r^2(k) + G_i^2(k)]} \tag{36}$$

Equations (32) and (33) are evaluated by breaking $F(z)$ into small straight-line segments and analytically integrating over the segments. This technique is known generally as the Filon Quadrature (*11*). For example, for the jth interval let $F_j(z) = a_j + b_j z$. For N data points (not necessarily equally spaced), Eq. (32) becomes

$$F_1(k) = (1/2\pi)^{1/2} \Bigg\{ \sum_{j=1}^{N-1} (a_j/k)[\sin(kz_{j+1}) - \sin(kz_j)] + \sum_{j=1}^{N-1} (b_j/k^2)[\cos(kz_{j+1}) + kz_{j+1} \sin(kz_{j+1}) - \cos(kz_j) - kz_j \sin(kz_j)] \Bigg\} \qquad k \neq 0 \tag{37}$$

In practice, both $F_1(k)$ and $F_2(k)$ are evaluated at equal intervals of k. By noting that $F_1(k) = F_1(-k)$ and $F_2(k) = -F_2(-k)$, the evaluation starts at $k = 0$ and simultaneously proceeds out in the positive and negative directions in k-space. The actual interval used in k-space varies because it is dependent on the value of k_{max} required for the evaluation of $F_1(k)$ and $F_2(k)$. Generally, the intervals in k were in the range $\pi/600 \leq \Delta k \leq \pi/20$. Since equal increments in k-space were selected, it was convenient to avoid multiple evaluations of the sine and cosine functions by means of expressions such as

$$\begin{aligned} \sin(k_{i+1}z_j) &= \sin(k_iz_j + \Delta kz_j) \\ &= \sin(k_iz_j)\cos(\Delta kz_j) + \cos(k_iz_i)\sin(\Delta kz_j) \end{aligned} \tag{38}$$

One of the major difficulties of the entire method, however, was determining the value of k_{max} out to which $F(k)$ should be evaluated. When $F(v)$ is a smooth analytical function, the magnitude of $F(k)$ goes to zero very smoothly as $|k|$ increases. Therefore $|F(k)|$ can be monitored and the generation terminated when $|F(k)|$ becomes suitably small. However, when $F(v)$ is actual experimental data, no such smooth behavior is encountered. In fact, rather slowly undulating oscillations are encountered as $|k|$ increases. This is due to two factors: (a) Noise and oscillations actually are present in $F(v)$; and (b) whenever a discontinuity appears in $F(v)$, due to the fact that the experimental data is chopped off at some arbitrary point before having a chance to approach zero asymptotically, oscillations will appear in the transform. Taking the transform of any simple function which is nonzero within a finite interval and zero outside of the interval will illustrate this point (*12*).

It is very difficult indeed to separate these two effects and determine the value of $|k|$ at which to terminate the evaluation of $F(k)$. If the numerical evaluation of $F(k)$ is performed out to values of $|k|$ that are too large, round-off errors will predominate because $F(k)$ is divided by $G(k)$, which itself goes to zero, resulting in a $0 \cdot \infty$ calculation. Termination of the evaluation of $F(k)$ at values of $|k|$ that are much too small will give poor results because much of the information is lost. Tung (*3*) used an empirical rule to determine the value of k_{max} and indicated that the results could be improved by varying this value for the particular problem.

A theoretical upper limit on k_{max} as given by the sampling theorem is

$$k_{max} = \pi/\Delta v \tag{39}$$

where Δv is the sampling interval. Some studies (*13*) have indicated that,

in practice, this should be closer to $0.1(\pi/\Delta v)$. However, a hard and fast rule appears difficult to ascertain.

A number of approaches has been suggested to overcome this problem (*10*). One approach is the use of a "spectral window" (*10*) to provide a weighting factor to force the tails of the chromatogram to approach zero smoothly. The use of a spectral window will be discussed further in Section 8 as well as the method used in practice to determine k_{max}.

The evaluation of $G(k)$ is made over the same range of k as used to determine $F(k)$. After $W(k)$ is evaluated, $W(v)$ is calculated using the same quadrature method that was used to evaluate $F(k)$. The spacing of the $W(v)$ function in v-space is determined by the spacing that was used in k-space. Generally, $F(v)$ curves covering narrow ranges of elution volume require evaluations in k-space out to large values of k (a coarse k-spacing) which in turn require very fine spacing in v-space for the $W(v)$ calculation. In this work, spacing was based on fractions of 600. Thus if the interval in k-space was $\pi/75$, then spacing in the corrected v-space was at count increments of 1/12.

5. THE CALIBRATION CURVE

Yau and Malone (*2*) derived a theoretical expression describing a relationship between molecular weight and elution volume. Their equation is of the form

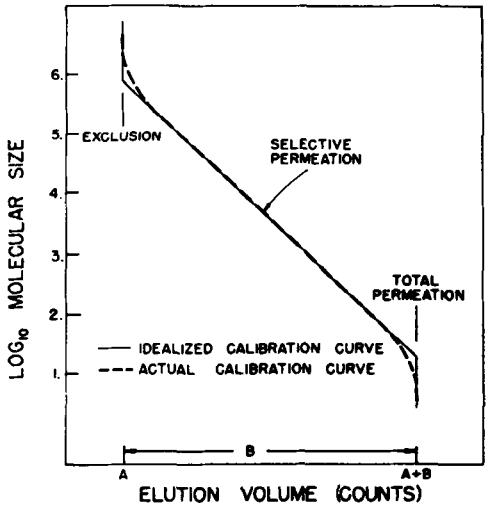

FIG. 2. Illustrative GPC calibration curve.

$$v = A + B\{(1/\sqrt{\pi}\psi)[1 - \exp(-\psi^2)] + \operatorname{erfc}(\psi)\} \quad (40)$$

where

$$\psi = M^D/C \quad (41)$$

The form of Eq. (40) has the characteristics of experimental GPC molecular weight calibration curves and has a number of convenient mathematical properties. If A, B, C, and D are treated as parameters, then Eq. (40) can be used to fit experimental molecular weight vs count data.

The value of A, once determined, is the effective exclusion volume and $A + B$ is the total volume as indicated in Fig. 2 taken from Ref. *14*. If sufficient data are not present in the steep portions of the curve at very high and very low elution volumes to determine A and B adequately, then this physical significance is lost.

Calibration curves such as shown in Fig. 2 are arbitrary to the extent that a particular molecular weight average such as $\bar{M}_v$, $\bar{M}_w$ or $(\bar{M}_w \cdot \bar{M}_n)^{\frac{1}{2}}$

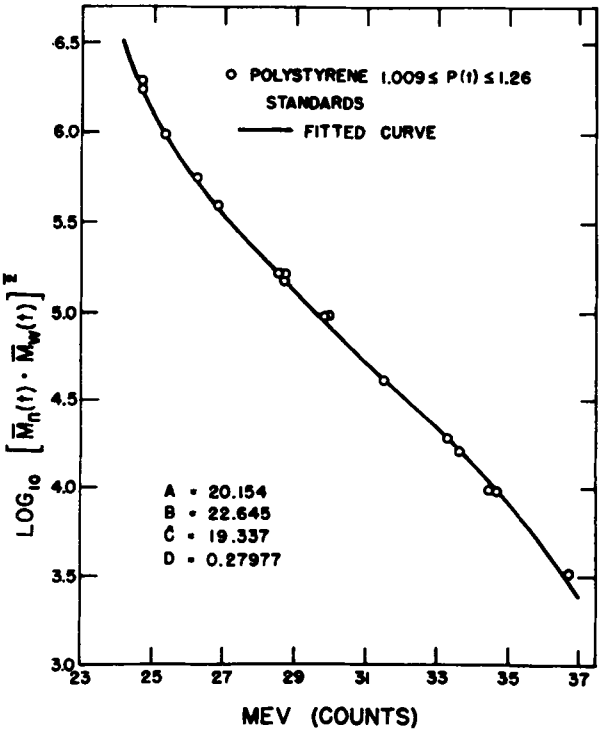

FIG. 3. Molecular weight calibration curve for polystyrene standards.

is associated with the peak elution volume (PEV) or mean elution volume (MEV).

Whatever is used, nevertheless, appears to be satisfactorily fit with Eq. (40). Figure 3 is a plot of the data given in Table 3 in which $(\bar{M}_n \cdot \bar{M}_w)^{\frac{1}{2}}$ is plotted vs MEV. Values* of A, B, C, and D were determined from a nonlinear least squares fit (*15*, *16*) of the data and are shown in Fig. 3.

Pickett, Cantow, and Johnson (*17*) have shown that $\bar{M}_n$ and $\bar{M}_w$ can be evaluated from

$$\bar{M}_n = \left[\int_{M_L}^{M_H} (1/M)(da/dM)\, dM\right]^{-1} \tag{42}$$

$$\bar{M}_w = \int_{M_L}^{M_H} M(da/dM)\, dM \tag{43}$$

where

$$(da/dM) = -\frac{C(v_M)}{\int_{V_L}^{V_H} C(v)\, dv} \cdot \frac{1}{(df/dv)_{v_M}} \cdot \frac{\log_{10} e}{M} \tag{44}$$

TABLE 3

Statistical and Molecular Weight Data for Polystyrene Standards Based on Normalized Chromatograms at 1ml/min Flow Rate

Run[a]	$10^{-3}\bar{M}_n(t)$	$10^{-3}\bar{M}_w(t)$	$P(t)$	MEV	m_2	m_3	m_4
181-189	1610	1900	1.18	24.65	2.487	5.833	33.05
181-190	1780	2145	1.21	24.67	2.463	5.690	31.61
181-188	773	867	1.12	25.31	1.686	3.458	17.25
181-187	404	507	1.26	26.27	1.801	3.164	17.36
181-186	392	411	1.05	26.84	1.833	3.390	19.06
181-184	170.9	179.3	1.05	28.52	0.933	0.457	4.224
181-183	164	173	1.05	28.68	0.642	0.473	2.119
184-211	160.6	162	$\leq$1.009	28.71	0.649	0.479	1.927
184-210	95.1	96	1.02	29.88	0.556	0.350	1.268
180-182	96.2	98.2	$\leq$1.009	29.90	0.540	0.335	1.394
184-209	42.12	42.5	$\leq$1.009	31.56	0.524	0.450	1.603
180-180	19.65	19.85	1.01	33.32	0.600	0.135	1.212
184-208	16.35	16.5	$\leq$1.009	33.61	0.406	0.128	0.572
184-207	9.91	10.0	$\leq$1.009	34.57	0.318	0.0471	0.316
180-179	9.70	10.3	1.06	34.73	0.662	0.283	1.701
180-178	3.18	3.53	$\leq$1.11	36.78	0.766	0.276	1.863

[a] Refer to (I.) for the commercial sources of the polystyrene standards.

* A Fortran IV computer program which makes use of Marquardt's algorithm to solve a set of nonlinear equations can be found in Ref. *16*.

The first term on the right-hand side of Eq. (44) is the normalized baseline-adjusted chromatogram height at elution volume v_M, where $C(v_M)$ is the raw chromatogram height at v_M and $\int_{V_L}^{V_H} C(v)\ dv$ is the area of the raw chromatogram. The second term on the right-hand side of Eq. (44) is the reciprocal of the slope of the calibration curve, $f(v) = \log_{10} M$. Equation (44) can be expressed as

$$(da/dM) = -[C(v_M)/\text{area}](dv/dM)v_M \tag{45}$$

From Eqs. (40) and (41)

$$(dv/dM)v_M = -(DB/\psi M\sqrt{\pi})[1 - \exp(-\psi^2)] \tag{46}$$

Since B, C, and D are always positive, $(dv/dM)v_M$ is always negative. Throughout this paper, $\bar{M}_n$ and $\bar{M}_w$ are determined by means of Eqs. (42), (43), (45), and (46).

6. EVALUATION OF THE INSTRUMENT SPREADING PARAMETERS

Before the Fourier transformed instrument spreading function defined by Eqs. (27) and (28) can be evaluated, it is necessary to determine the values of μ_2, μ_3, and μ_4 as a function of elution volume. In principle, these parameters can be determined from a knowledge of $\bar{M}_n(t)$, $\bar{M}_w(t)$, and $[\eta](t)$ or $\bar{M}_v(t)$. However, in this paper it shall be assumed that only $\bar{M}_n(t)$ and $\bar{M}_w(t)$ are available. In addition an assumption shall be made regarding the nature of the corrected chromatogram for narrow MWD standards.

If the chromatograms of the characterized standard polymer samples cover narrow ranges of elution volume, it can be assumed that (a) μ_2, μ_3, and μ_4 are slowly varying functions of elution volume and will be reasonably constant over this elution volume range, and (b) the calibration curve will be reasonably linear over this elution volume range. Under these assumptions, it has been shown in (I.) that the following correction equations are applicable.

$$\frac{\bar{M}_n(t)}{\bar{M}_n(\infty)} = \exp(\alpha^2/2)\{1 + \sqrt{\beta_1}\alpha^3/6 + (\alpha^4/24)(\beta_2 - 3)\} \tag{47}$$

$$\frac{\bar{M}_w(\infty)}{\bar{M}_w(t)} = \exp(\alpha^2/2)\{1 - \sqrt{\beta_1}\alpha^3/6 + (\alpha^4/24)(\beta_2 - 3)\} \tag{48}$$

where

$$\alpha = D_2\sqrt{\mu_2} \tag{49}$$

$$\beta_1 = \mu_3^2/\mu_2^3 \tag{50}$$

$$\beta_2 = \mu_4/\mu_2^2 \tag{51}$$

D_2 is the slope of the $\log_e M$ vs elution volume calibration curve at a specified elution volume v_s and is given by

$$D_2 = (d \log_e M/dv)_{v_s} = [M(dv/dM)_{v_s}]^{-1} \tag{52}$$

In terms of the parameters of the Yau-Malone function, D_2 is expressed as

$$D_2 = -(\sqrt{\pi}\,\psi/DB)[1 - \exp(-\psi^2)]^{-1} \tag{53}$$

Addition of Eqs. (47) and (48) results in an expression for the fundamental parameter α.

$$\alpha^2 = 2 \log_e \left\{\frac{[\bar{M}_n(t)/\bar{M}_n(\infty)] + [\bar{M}_w(\infty)/\bar{M}_w(t)]}{2[1 + (\alpha^4/24)(\beta_2 - 3)]}\right\} \tag{54}$$

Subtracting Eq. (48) from Eq. (47) and combining the result with Eq. (54) yields an expression for the fundamental parameter β_1.

$$\sqrt{\beta_1} = (6/\alpha^3)[1 + (\alpha^4/24)(\beta_2 - 3)] \times \left\{\frac{[\bar{M}_n(t)/\bar{M}_n(\infty)] - [\bar{M}_w(\infty)/\bar{M}_w(t)]}{[\bar{M}_n(t)/\bar{M}_n(\infty)] + [\bar{M}_w(\infty)/\bar{M}_w(t)]}\right\} \tag{55}$$

Equations (54) and (55) are two equations in the three unknowns α, β_1, and β_2. For the third equation, consider the relationship between the fourth moment of the observed and corrected chromatogram as shown in Table 1.

$$m_4^* = m_4 - 6\mu_2 m_2 + 6\mu_2^2 - \mu_4 \tag{56}$$

If the corrected chromatogram for the standard is assumed to be nearly Gaussian in shape, then $m_4^* = 3m_2^*$. Using this assumption along with the relation $m_2^* = m_2 - \mu_2$ in Eq. (56) results in

$$\mu_4 - 3\mu_2^2 = m_4 - 3m_2^2 \tag{57}$$

Combining Eq. (57) with Eqs. (49) and (51) leads to the necessary third equation

$$(\alpha^4/24)(\beta_2 - 3) = (D_2^4/24)(m_4 - 3m_2^2) \tag{58}$$

Use of Eq. (58) in (54) and (55) leads to expressions for α and β_1 in terms of quantities that can be determined by measurement or calculation.

$$\alpha^2 = 2 \log_e \left\{ \frac{[\bar{M}_n(t)/\bar{M}_n(\infty)] + [\bar{M}_w(\infty)/\bar{M}_w(t)]}{2[1 + (D_2^4/24)(m_4 - 3m_2^2)]} \right\} \tag{59}$$

$$\alpha^3 \sqrt{\beta_1} = 6[1 + (D_2^4/24)(m_4 - 3m_2^2)] \times \left\{ \frac{[\bar{M}_n(t)/\bar{M}_n(\infty)] - [\bar{M}_w(\infty)/\bar{M}_w(t)]}{[\bar{M}_n(t)/\bar{M}_n(\infty)] + [\bar{M}_w(\infty)/\bar{M}_w(t)]} \right\} \tag{60}$$

It is important to note that α is negative due to the negativity of D_2 in Eq. (49).

The calibration procedure to obtain μ_2, μ_3, and μ_4 as a function of elution volume is described below. The raw data of the standards used in this procedure are the data shown in Table 3 along with the corresponding raw elution volume curves. The experimental GPC conditions and procedures used for the generation of the raw chromatograms have been described previously in (I.).

(a) The raw $\bar{M}_n(t)$ vs MEV and $\bar{M}_w(t)$ vs MEV data sets in Table 3 are each fit to the functional form of the Yau-Malone Eq. (40). The smooth values $\bar{M}_n(t)_s$ and $\bar{M}_w(t)_s$ are calculated from the fitted functions. The results are shown in Table 4 with the subscript s denoting smooth values.

(b) The infinite resolution molecular weight calibration curve is obtained by using Eq. (40) to fit $[\bar{M}_n(t) \cdot \bar{M}_w(t)]^{1/2}$ vs MEV data. Values

TABLE 4

Smooth Values of Molecular Weight for Polystyrene Standards

Run	MEV	$10^{-3}\bar{M}_n(t)_s$	$10^{-3}\bar{M}_w(t)_s$	$P(t)_s$	$10^{-3}\bar{M}_n(\infty)_s$	$10^{-3}\bar{M}_w(\infty)_s$	$P(\infty)_s$
181-189	24.65	1510	1780	1.18	925	3090	3.34
181-190	24.67	1490	1740	1.17	913	3020	3.31
181-188	25.31	934	1100	1.18	661	1580	2.39
181-187	26.27	513	576	1.12	408	725	1.78
181-186	26.84	372	418	1.12	317	490	1.55
181-184	28.52	166	174	1.05	152	186	1.22
181-183	28.68	155	162	1.05	142	173	1.22
184-211	28.71	152	158	1.04	141	170	1.21
184-210	29.88	89.2	92.7	1.04	85.1	96.8	1.14
180-182	29.90	89.2	92.5	1.04	85.0	96.2	1.13
184-209	31.56	43.7	43.8	1.002	41.7	44.7	1.07
180-180	33.32	19.5	19.6	1.005	18.6	20.4	1.10
184-208	33.61	17.0	17.1	1.006	15.9	17.8	1.12
184-207	34.57	10.5	11.0	1.05	9.55	11.2	1.17
180-179	34.73	9.78	10.0	1.02	8.91	10.5	1.18
180-178	36.78	2.89	3.24	1.12	2.40	3.39	1.41

of the Yau-Malone parameters are given together with the fitted curve in Fig. 3.

(c) The infinite resolution calibration curve and the raw chromatograms of the standards are used to calculate $\bar{M}_n(\infty)$ and $\bar{M}_w(\infty)$. These values are again smoothed by fitting to Eq. (40). Values of $\bar{M}_n(\infty)_s$ and $\bar{M}_w(\infty)_s$ are shown in Table 4.

(d) The values of $\bar{M}_n(t)_s$, $\bar{M}_w(t)_s$, $\bar{M}_n(\infty)_s$, and $\bar{M}_w(\infty)_s$ together with the statistics of the standards given in Table 3 are used to find the value of α^2 from Eq. (59) at each MEV. Equation (53) is used to evaluate D_2 at each MEV. Plots of α and α^2 vs MEV are shown in Fig. 4 and a plot of D_2 vs MEV is shown in Fig. 5.

(e) Values of μ_2 are calculated at equal increments of elution volume using Eq. (49) and Fig. 5. These results are given in Table 5 and plotted in Fig. 6.

(f) Values of $\sqrt{\beta_1}$ are calculated at each MEV using Eqs. (60) and

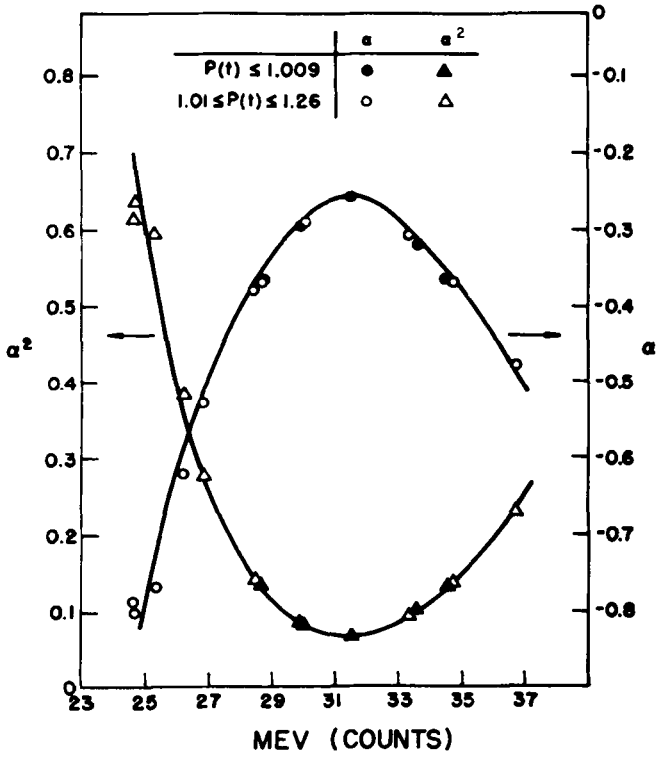

FIG. 4. α and α^2 vs MEV.

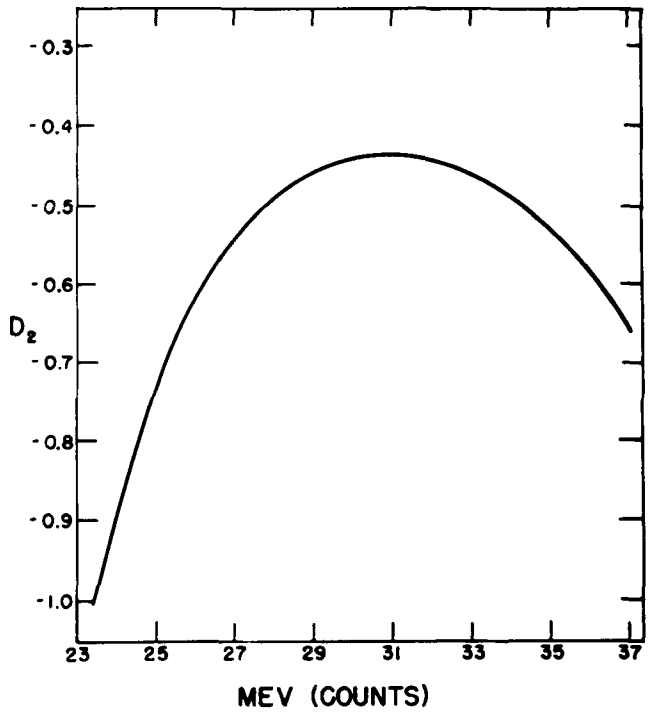

FIG. 5. D_2 vs MEV.

TABLE 5

Interpolated Values of μ_2, μ_3, and μ_4 at Equal Increments of the Mean Elution Volume

MEV	μ_2	μ_3	μ_4
23	0.825	0.970	19.1
24	0.950	0.695	19.0
25	1.05	0.270	17.1
26	1.05	0.160	13.2
27	0.927	0.047	8.15
28	0.750	0.00	4.32
29	0.593	0.0145	2.22
30	0.465	0.0346	1.15
31	0.397	−0.0750	0.706
32	0.370	−0.213	0.550
33	0.425	−0.500	0.650
34	0.510	−0.890	0.859
35	0.550	−1.18	0.966
36	0.595	−1.52	1.10
37	0.580	−1.63	1.01

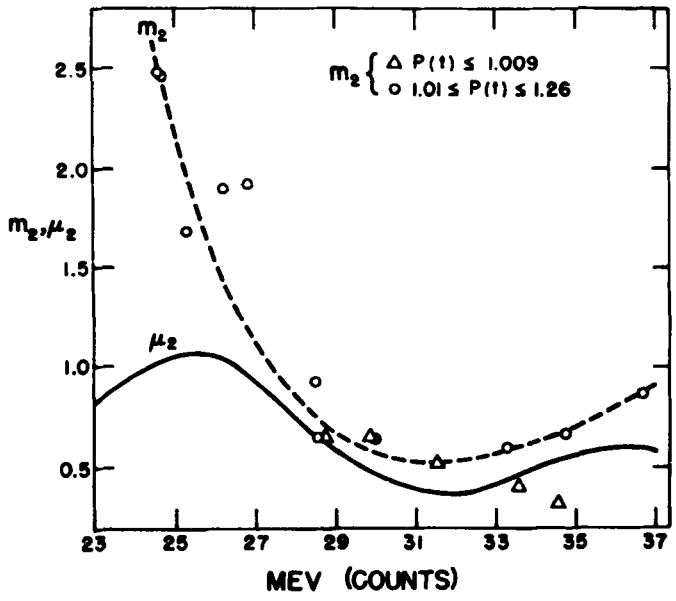

FIG. 6. m_2 and μ_2 vs MEV.

(53) and Fig. 4. Then values of μ_3 at equal increments of elution volume are obtained from a plot of $\sqrt{\beta_1}$ vs MEV in Fig. 7, Eq. (50), and Fig. 6.

(f) Values of μ_3 at equal increments of elution volume are given in Table 5 and plotted in Fig. 8.

(g) Values of β_2 are calculated at each MEV from Eqs. (58) and (53) and Fig. 4. Then values of μ_4 at equal increments of elution volume are obtained from a plot of β_2 vs MEV in Fig. 9, Eq. (51), and Fig. 6. Values of μ_4 at equal increments of elution volume are given in Table 5 and plotted in Fig. 10.

Several points in the above procedure are worthy of note. (a) The smoothing operations on $\bar{M}_n(t)$, $\bar{M}_w(t)$, $\bar{M}_n(\infty)$, and $\bar{M}_w(\infty)$ eliminated much of the scatter in the plots of μ_2, μ_3, and μ_4 vs MEV. (b) The entire calibration procedure was rather arbitrary because, in principle, $\bar{M}_w(t)$ vs PEV could have been used instead of $[\bar{M}_n(t) \cdot \bar{M}_w(t)]^{\frac{1}{2}}$ vs MEV. However, use of $\bar{M}_w(t)$ vs PEV gave less satisfactory numerical values of β_1.

The rather surprising shape of the μ_2 vs MEV curve in Fig. 6 can perhaps be justified by plotting values of m_2 on the same plot. Since m_2^* must always be positive, this implies that $m_2 > \mu_2$. With the exception of two points of the ultranarrow recycle polystyrene standards, the

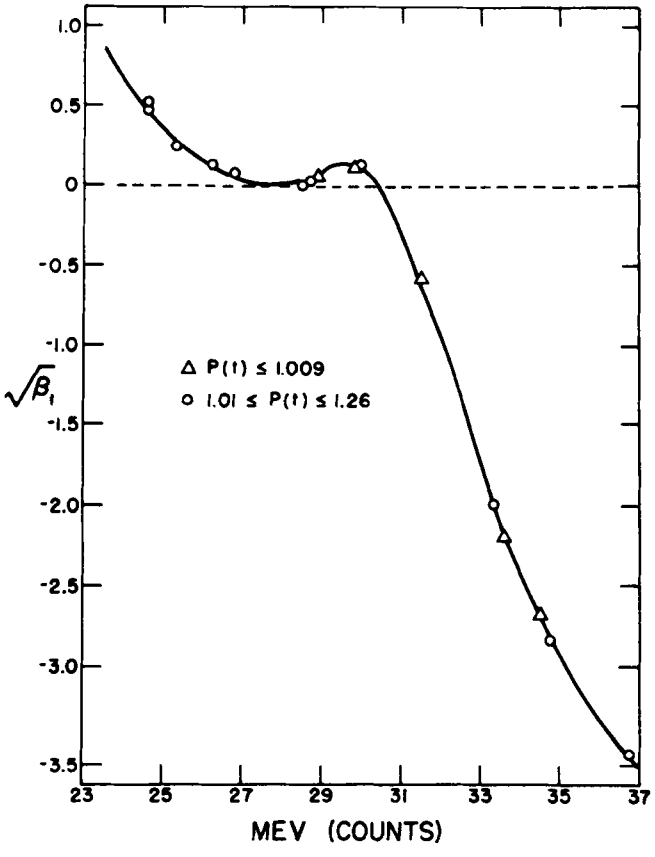

FIG. 7. $\sqrt{\beta_1}$ vs MEV.

values of m_2 are, in fact, greater than μ_2 within experimental errors.

Similar reasoning can be applied to Fig. 10. Since $m_4^* > 0$, it follows from Eq. (56) that

$$m_4^* + \mu_4 = m_4 - 6\mu_2 m_2 + 6\mu_2^2 > \mu_4 \tag{61}$$

Generally, $m_4^* \geq 0.03$ over most of the elution volume range. Therefore, Eq. (61) holds. Figure 10 illustrates that, generally, $m_4^* \ll \mu_4$ because many of the experimental data points are almost indistinguishable from the μ_4 curve.

It is difficult to assess the effect of the use of the approximation given by Eq. (58) except to note that, generally, $D_2^4(m_4 - 3m_2^2)/24 \ll 1$.

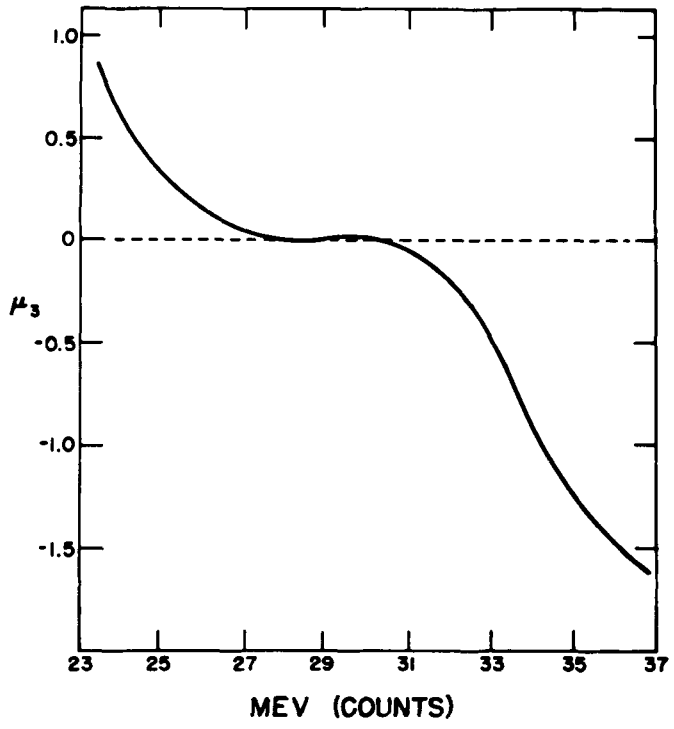

FIG. 8. μ_3 vs MEV.

However, when $|D_2|$ begins to climb rapidly in the low MEV region, the above inequality is no longer valid and the approximation made in Eq. (58) may introduce serious errors in the determination of μ_2, μ_3, and μ_4.

Over some regions of elution volume the values of β_1 and β_2 fall outside the unimodal and positive definite regions of the Gram-Charlier curves as indicated in Fig. 1. However, this does not necessarily mean that the instrument spreading function is predicting unrealistic values over the elution volume range of the sample. Unrealistic values of $G(v\text{-}y)$ that do occur over the elution volume range of the sample may be so small that they have no practical significance with respect to the values of $W(v)$ generated by the numerical Fourier transform method. Consider, for example, that the normalized observed chromatogram can be described by the skewed Gaussian function

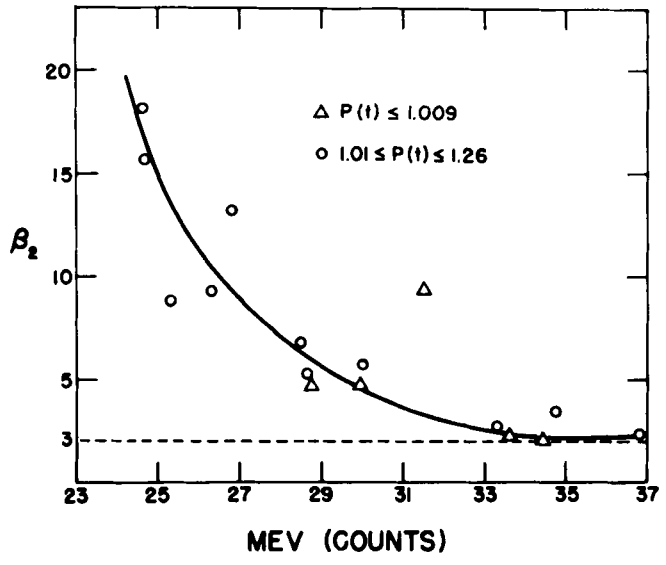

FIG. 9. β_2 vs MEV.

$$F(v) = (1/2\pi m_2)^{1/2} \exp[-(v-\mu)^2/2m_2] \times \{1 + (C_3/3!)H_3[(v-\mu)/\sqrt{m_2}] + (C_4/4!)H_4[(v-\mu)/\sqrt{m_2}]\} \quad (62)$$

where

$$C_3 = m_3/m_2^{3/2} \quad (63)$$

$$C_4 = m_4/m_2^2 - 3 \quad (64)$$

Then

$$F(k) = (1/\sqrt{2\pi}) \exp(-k^2 m_2/2)\{1 + (C_3/3!)(ik\sqrt{m_2})^3 + (C_4/4!)k^4 m_2^2\} \quad (65)$$

From Eqs. (27), (28), and (14)

$$W(k) = (1/\sqrt{2\pi}) \exp\left[\frac{-k^2(m_2 - \mu_2)}{2}\right] \left\{\frac{1 + \frac{C_3}{3!}(ik\sqrt{m_2})^3 + \frac{C_4}{4!}k^4 m_2^2}{1 + \frac{A_3}{3!}(ik\sqrt{\mu_2})^3 + \frac{A_4}{4!}k^4\mu_2^2}\right\} \quad (66)$$

Equation (66) contains an exponential in m_2^* multiplied by a ratio of polynomials in the parameters β_1 and β_2 through the coefficients A_3 and

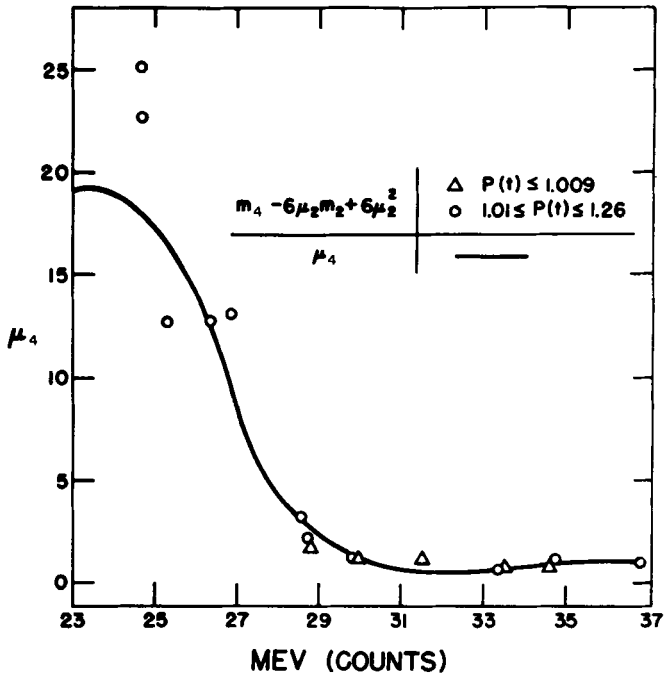

FIG. 10. μ_4 and $m_4 - 6\mu_2 m_2 + 6\mu_2^2$ vs MEV.

A_4, and in the parameters m_3 and m_4 through the coefficients C_3 and C_4. If m_2^* ($m_2^* = m_2 - \mu_2$) is large, it is not necessary to go out too far in k-space in order for the exponential term to wash out the effect of the bracketed term in Eq. (66) and force $|W(k)|$ to go to zero. On the other hand, when m_2^* is small, it is necessary to go out farther in k-space. Then, the effect of noise in the numerical $F(v)$ data and round-off errors tend to be greatly magnified at large values of k and prevents $|W(k)|$ from going to zero. If $|W(k)|$ is poorly bounded, $W(v)$ will tend to have unrealistic values manifested by large positive and negative oscillations.

7. TEST RESULTS—ANALYTICAL DATA

In order to check the numerical procedures used in the Fourier transform method, two analytical functions were chosen for study. The first test function was designed to check the functioning of the dispersion, skewing, and flattening parameters. The observed chromatogram was

described by a skewed Gaussian function which transformed to a corrected chromatogram that was described by a pure Gaussian function. The pure Gaussian function in k-space is given by

$$W(k) = (1/2\pi)^{1/2} \exp(-k^2 m_2^*/2) \tag{67}$$

Using Eqs. (27), (28), and (14), the following expression can be derived for $F(v)$

$$F(v) = (1/2\pi m_2)^{1/2} \exp[-(v-\mu)^2/2m_2]\{1 + (\mu_3/6m_2^{3/2})H_3[(v-\mu)/\sqrt{m_2}] + \{(\mu_4 - 3\mu_2^2)/24m_2^2\}H_4[(v-\mu)/\sqrt{m_2}\} \tag{68}$$

where

$$m_2 = m_2^* + \mu_2 \tag{69}$$

$F(v)$ was generated over the range $18 \leq v \leq 42$ about $\mu = 30$ with $\Delta v = 0.1$.

Equation (67) immediately suggests a method for determining a means of estimating the value of k_{max} in k-space out to which $F(k)$ should be evaluated. If k_{max} is such that $\exp(-k^2 m^*/2) = 5 \times 10^{-6}$, then

$$k_{max} = [-2 \log_e (5 \times 10^{-6})/(m_2 - \mu_2)]^{1/2} \tag{70}$$

This was the method used to estimate k_{max} throughout this paper. If $|F(k)|$ reached a minimum value of 5×10^{-5} before k_{max} was encountered, then that value of k was the largest value of k used.

Table 6 illustrates the performance of the numerical procedures used in the computer program to transform the test $F(v)$ function in Eq. (68) to the corrected Gaussian function for varying values of m_2^*. As m^* decreased the value of k_{max} increased, and larger values of Δk were required to proceed to the desired value of k_{max} because a fixed number of computer storage locations were allotted for Δk-increments in k-space. In all cases the minimum value of $|F(k)|$ was encountered before k_{max} was reached. When m_2^* was small, this resulted in $|W(k)|$, the critical quantity, being too large at the termination of the generation. Consequently, there was a loss in the accuracy of the computation as measured by the statistics.

It can be argued that a better procedure would be to always allow the computation of $F(k)$ to proceed until k_{max} is encountered. However, very small values of $|F(k)|$ would be used and roundoff and integration errors would begin to predominate. With the above method there is a

TABLE 6

Results for Analytical Test Functions

Statistic	Test function, Eq. (68), $\mu_3 = -0.7$, $\mu_4 = 4.5$, fixed values of m_2^*				Tung's function Eq. (71) $H = 0.4$
	1.0	0.5	0.3	0.1	
Raw[a] area	1.0000	1.0000	1.0000	0.99999	0.99999
Corrected[b] area	0.99977	1.0003	1.0025	1.0266	0.99959
Raw MEV	30.000	30.000	30.000	30.000	27.40
Corrected MEV	30.000	30.000	30.000	30.000	27.39
m_2	2.0000	1.5000	1.3000	1.1000	16.49
μ_2	1.0000	1.0000	1.0000	1.0000	3.125
Predicted[c] m_2^*	1.0000	0.50000	0.30001	0.10003	13.37
Corrected m_2^*	1.0031	0.50442	0.31519	0.11245	13.60
m_3	−0.69952	−0.69980	−0.69972	−0.69984	10.37
μ_3	−0.7	−0.7	−0.7	−0.7	0
Predicted m_3^*	0.00048	0.00019	0.00028	0.00016	10.37
Corrected m_3^*	0.00017	0.000058	0.000016	0.000003	10.32
m_4	13.500	8.2510	6.5696	5.1298	679.64
μ_4	4.5000	4.5000	4.5000	4.5000	29.29
Predicted m_4^*	2.9998	0.75098	0.26960	0.029583	399.60
Corrected m_4^*	3.0555	0.76979	0.34160	0.029843	397.28
k_{max} from Eq. (70)	4.94	6.98	9.02	15.62	1.35
Δk	$\pi/50$	$\pi/40$	$\pi/30$	$\pi/20$	$\pi/20$
$\lvert F(k)\rvert_{min}$[d]	5×10^{-6}	5×10^{-6}	5×10^{-6}	5×10^{-6}	5×10^{-6}
k_{max} used[e]	3.39	4.00	4.39	4.86	1.35
$\lvert W(k)\rvert$ at k_{max} used	0.00125	0.00713	0.0215	0.119	0.00334

[a] All the statistics preceded by the word "raw" are those calculated from $F(v)$, the normalized observed chromatogram.

[b] All the statistics preceded by the word "corrected" are those calculated from the $W(v)$ obtained from $F(v)$ by the numerical Fourier transformation procedures.

[c] All the statistics preceded by the word "predicted" are those calculated from the relations in Table 2.

[d] $\lvert F(k)\rvert_{min}$ was set equal to 5×10^{-6}.

[e] k_{max} used refers to the actual largest value of k used to evaluate $F(k)$.

limitation on the value of m_2^* that can be handled with accuracy. With experimental data the value of k_{max} is always used because noise and oscillations prevent $|F(k)|$ from ever reaching any reasonably small minimum value of $|F(k)|$. Figure 11 is a plot of $F(v)$, the true $W(v)$, and the calculated $W(v)$ obtained from $F(v)$ for the case where $m_2^* = 0.3$, $\mu_2 = 1.0$, $\mu_3 = -0.7$, and $\mu_4 = 4.5$.

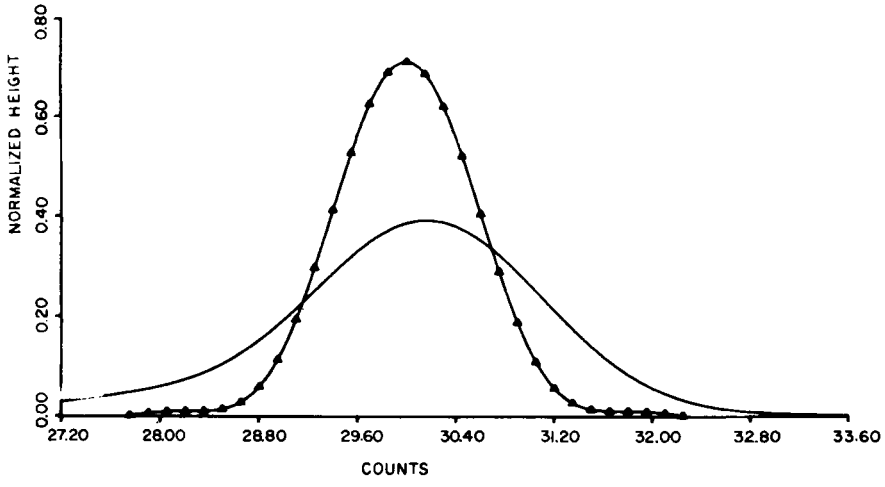

FIG. 11. Test function-skewed Gaussian for $m_2^* = 0.3$, $\mu_2 = 1$, $\mu_3 = -0.7$, $\mu_4 = 4.5$: $-F(v)$ from Eq. (68), ▲ corrected $W(v)$. Note true values of $W(v)$ calculated from Gaussian function are not shown because they are coincident with the corrected values.

The second function studied was suggested by Tung (*3*) and is

$$F(v) = \frac{0.325H}{\sqrt{\pi[(0.325)^2 + H^2]}} \left\{0.6 \exp\left[-\frac{(0.325)^2H^2(v-25)^2}{(0.325)^2 + H^2}\right] + 0.4 \exp\left[-\frac{(0.325)^2H^2(v-31)^2}{(0.325)^2 + H^2}\right]\right\} \quad (71)$$

with $H = 0.4$. Note that

$$H = 1/\sqrt{2\mu_2} \quad (72)$$

The corrected chromatogram is

$$W(v) = \frac{0.325}{\sqrt{\pi}} \times \{0.6 \exp[-(0.325)^2(v-25)^2] + 0.4 \exp[-(0.325)^2(v-31)^2]\} \quad (73)$$

$F(v)$ was generated over the range $12 \leq v \leq 44$ with $\Delta v = 0.1$. The numerical results for this case are also shown in Table 6. A plot of $F(v)$, the true $W(v)$, and the calculated $W(v)$ obtained from $F(v)$ are shown in Fig. 12.

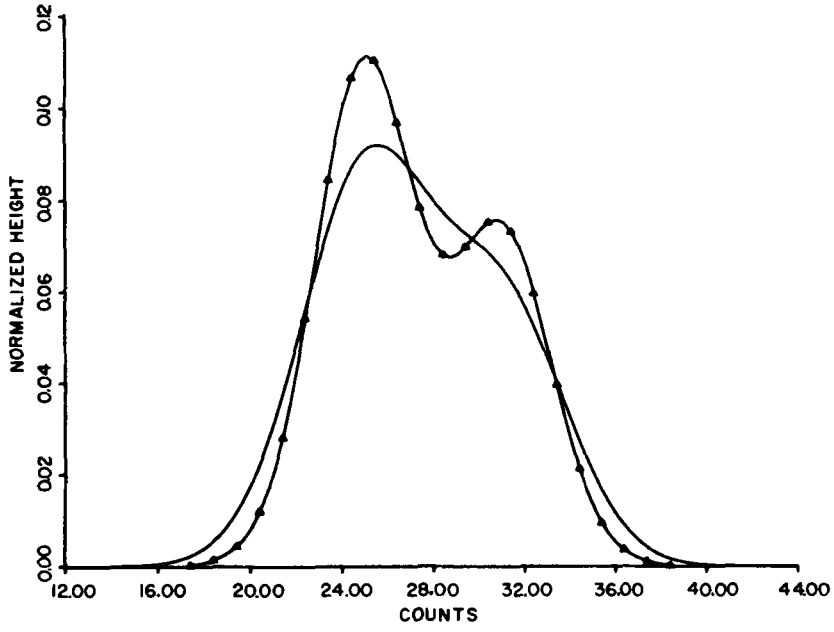

FIG. 12. Tung's analytical test function for $H = 0.4$, $\mu_3 = 0$, $\mu_4 = 29.29$: $-F(v)$ from Eq. (71), ▲ corrected $W(v)$. Note true values of $W(v)$ calculated from Eq. (73) are not shown because they are coincident with the corrected values.

8. TEST RESULTS—EXPERIMENTAL DATA

In order to test the method on actual experimental data, five samples were selected. The first was a broad MWD standard. The other four were mixtures prepared by mixing three of the calibration standards together in various proportions by weight. The resulting polyblends were narrow in MWD and distinctly multimodal. These five samples are described in Table 7.

Since the raw data tended to be noisy at the tails, the "spectral window" shown in Fig. 13 was used to smooth the tails of the chromatogram. The window used was an extended cosine-bell data window (*10*). This window generated a "factor" between 0 and 1 by which the raw data was multiplied over the first and last 10% of the total number of data points. The middle 80% of the total number of data points was unchanged.

TABLE 7

Composition and Molecular Weight Data for Experimental Test Samples

Run[a]	Wt%[b] composition	$10^{-3}\bar{M}_n(t)$[c]	$10^{-3}\bar{M}_w(t)$	$P(t)$
181-185	NBS-706	136.5	257.8	1.889
196-302-1	0/50/50	64.9	74.6	1.15
196-305-1	75/25/0	23.1	27.6	1.20
196-306-1	25/75/0	35.6	43.2	1.21
196-308-1	16.7/33.3/50	48.8	69.4	1.42

[a] All samples were run at a flow rate of 1 ml/min.

[b] The wt% of each polystyrene standard in the mixture refers to the standards with the run numbers in the following order: 180-180, 180-181, and 180-182.

[c] The true values, $\bar{M}_n(t)$, $\bar{M}_w(t)$, and $P(t)$ of the mixtures were calculated from the true values of the individual components and compositions of the mixtures.

The distance in k-space, out to which $F(k)$ was evaluated, was determined from Eq. (70) with μ_2 evaluated at the MEV of the sample. Values of $W(v)$, which were generated out in each direction from v_0, generally became negative at the ends of the chromatogram. If more than five negative values were encountered, this was used as an indication to terminate the evaluation of $W(v)$. However, this criterion allowed

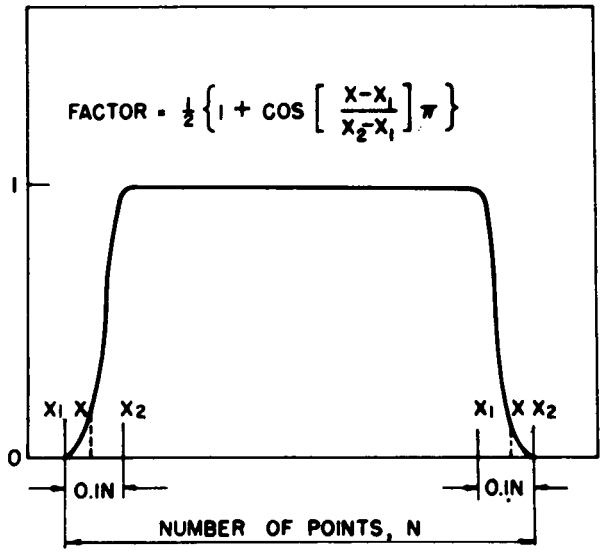

FIG. 13. An extended cosine-Bell data window.

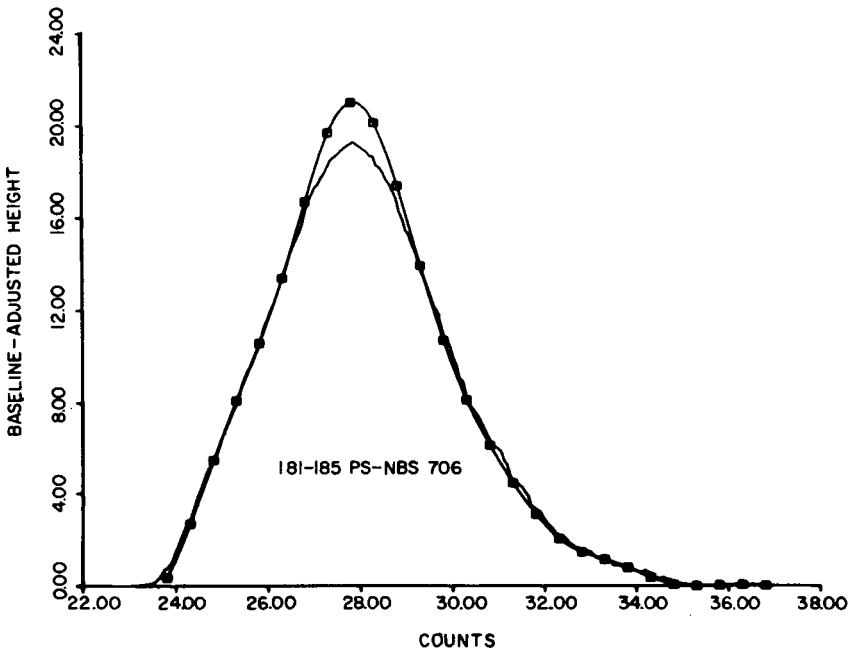

FIG. 14. Observed $\{-F(v)\}$ and corrected $\{\boxminus, W(v)\}$ chromatograms for sample 181-185.

the generation of completely separated peaks. All negative values of $W(v)$ were set equal to zero.

Figures 14–18 are plots of $F(v)$ and $W(v)$ for the samples shown in Table 7. The variations of the μ_2, μ_3, and μ_4 with elution volume that were used in the calculations are given in Table 5. Linear interpolation was used between the tabulated points.

Values of $\bar{M}_n(\infty)$ and $\bar{M}_w(\infty)$ obtained from the calibration curve of Fig. 3 and the observed chromatogram $F(v)$, and values of $\bar{M}_n(t)_w$ and $\bar{M}_w(t)_w$ obtained from the corrected chromatogram $W(v)$ and the calibration curve of Fig. 3 are shown in Table 8. For comparison purposes the values of μ_2, μ_3, and μ_4 were evaluated at the MEV's and were subsequently used to evaluate $\bar{M}_n(t)_E$ and $\bar{M}_w(t)_E$ from Eqs. (47) and (48).

As can be seen from a study of Table 8, the areas of $W(v)$ are almost always consistently higher than those of $F(v)$. When the parameters μ_2, μ_3, and μ_4 are functions of elution volume, it is difficult to prove mathematically that the area of the raw chromatogram is equal to the area of the corrected chromatogram. From Eq. (1)

$$\int_{-\infty}^{\infty} F(v)\,dv = \int_{-\infty}^{\infty}\int_{-\infty}^{\infty} G(v-y)W(y)\,dy\,dv \qquad (74)$$

The use of the convolution theorem or a transformation of variables to interchange the order of integration with respect to y and v to prove the area equality requires the constancy of μ_2 with v. The same argument leads to the conclusion that none of the relationships of Table 2 strictly hold. However, it should be noted from Table 8 and Fig. 16 that in the case of sample 196-305-1, where the sample was in the range of reasonable constancy of the μ_n's, the areas indeed gave a reasonable check. From physical arguments the areas must check within experimental errors because the area under the chromatogram represents a certain number of milligrams of material that has passed through the GPC columns and the differential refractometer detector.

Table 8 also shows that the evaluation of $F(k)$ always proceeded out to the value of k_{max}. The minimum value of $|F(k)|$ was not encountered first because of the noise and oscillations in the data. Since there was

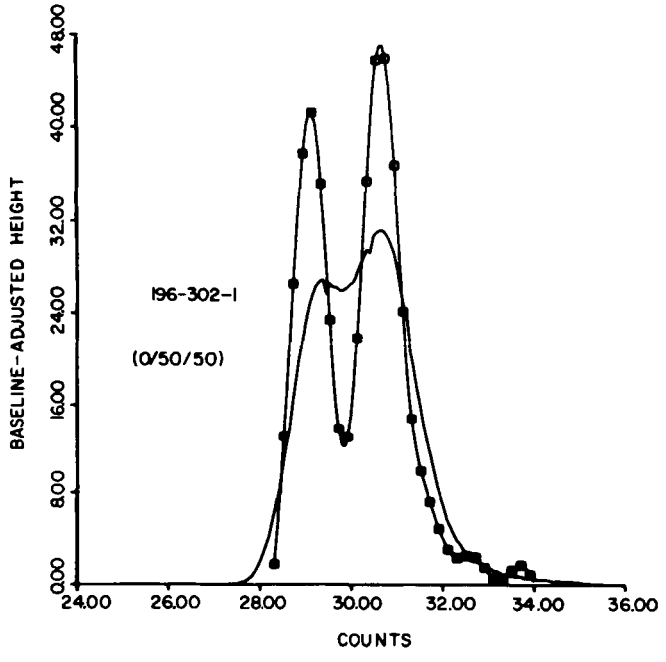

FIG. 15. Observed {$-F(v)$} and corrected {⊟, $W(v)$} chromatograms for sample 196-302-1.

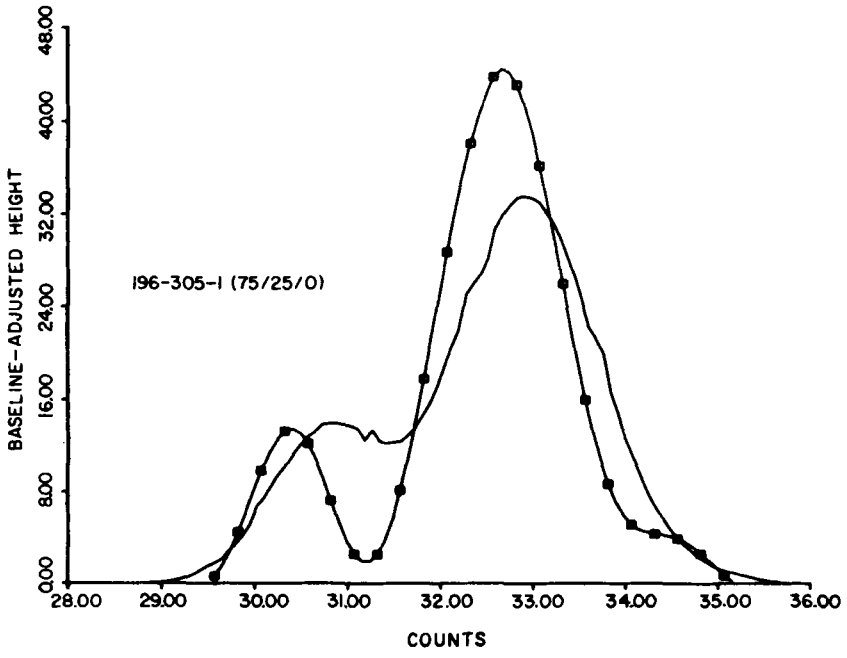

FIG. 16. Observed $\{-F(v)\}$ and corrected $\{\boxminus, W(v)\}$ chromatograms for sample 196-305-1.

considerable doubt that the value of k_{max} used was adequate, the value of k_{max} was increased for each of the samples to 1½ times the value indicated in Table 8. Not much effect was observed in the broad MWD sample. However, greater resolution of the components in the 196-series of samples (small m_2^*'s) was achieved. How realistic this increased resolution was is open to question. The "correct" value of k_{max} to use is unresolved and remains a major area for further investigation.

9. CONCLUSIONS

Based on this study several conclusions can be made.

(a) The instrument spreading function given by Eq. (5) is useful for characterizing the dispersion, skewing, and flattening effects encountered in raw GPC chromatograms due to the imperfect resolution by the GPC columns. It is limited, however, to applications where

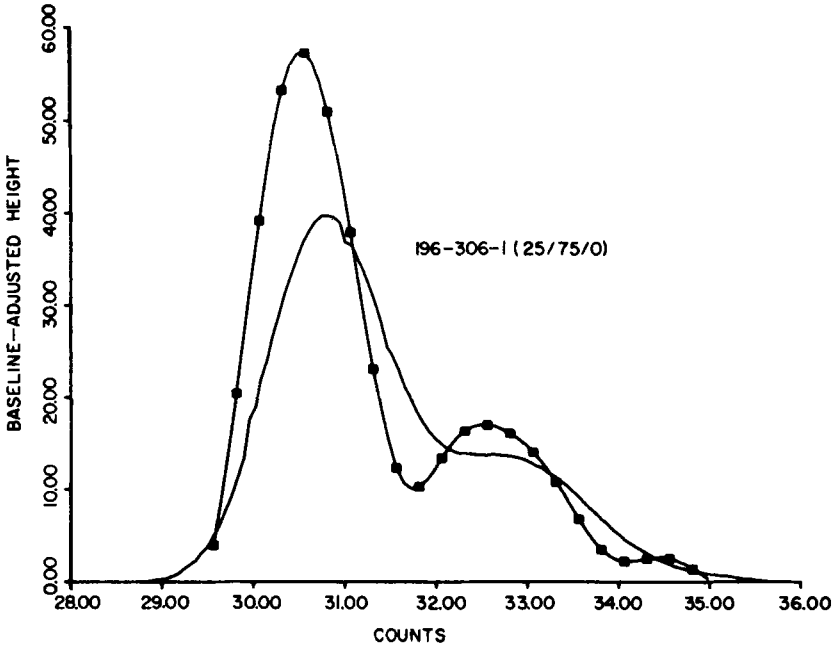

FIG. 17. Observed {—$F(v)$} and corrected {⊟, $W(v)$} chromatograms for sample 196-306-1.

m_2^* is large enough to "wash out" large oscillations caused by large values of β_1 and β_2 relative to the values of m_2, m_3, and m_4.

(b) The Yau-Malone function given by Eq. (40) is a flexible and useful equation for the fitting of molecular weight vs elution volume data.

(c) The Fourier transform method, while it can be demonstrated to work well on analytically generated data, has a number of problems associated with it when applied to actual experimental data. At this time these problems appear to be associated with two major considerations: (1) It is not clear how far out in k-space to go in generating $F(k)$ and hence $W(k)$. Equation (70), while probably qualitatively useful, does not appear to be adequate. (2) It is not clear how serious are the assumptions of the constancy of the parameters μ_2, μ_3, and μ_4 with elution volume in situations where they are reasonably strong functions of elution volume and/or the sample covers a broad range of elution volume.

(d) The Fourier transform method is useful in qualitatively resolving

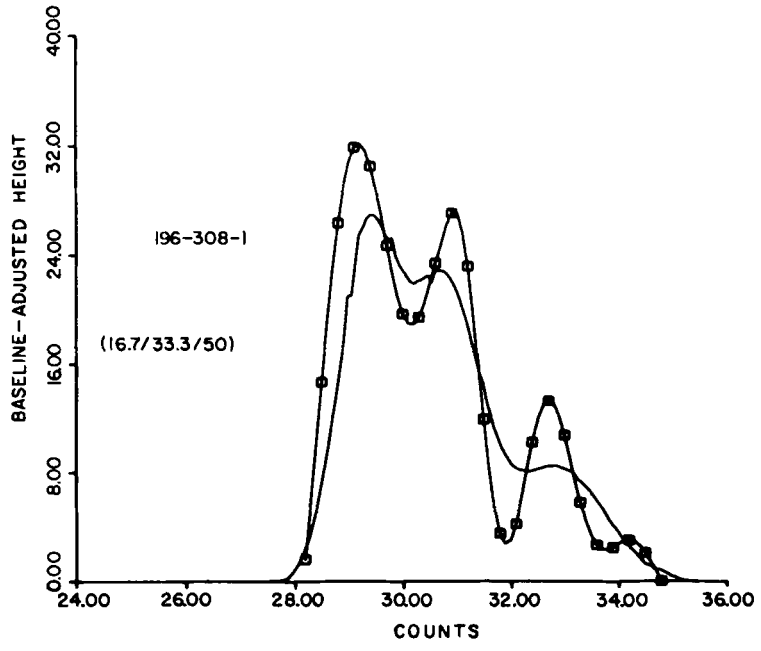

FIG. 18. Observed {—$F(v)$} and corrected {⊟, $W(v)$} chromatograms for sample 196-308-1.

peaks.

(c) The calibration procedure used, though arbitrary, gives values of the parameters μ_2, μ_3, and μ_4 which are physically reasonable. When the sample is a narrow MWD sample, then Eqs. (47) and (48) can be used, with parameters evaluated at the MEV of the sample, to evaluate $\bar{M}_n(t)$ and $\bar{M}_w(t)$. When the samples are broad in MWD, the adequacy of Eqs. (47) and (48) are in doubt because of the variability of the μ_n's with elution volume.

10. SUGGESTIONS FOR IMPROVEMENTS IN THE CALIBRATION AND NUMERICAL PROCEDURES*

The use of Eqs. (47) and (48) tied together the determination of the instrument spreading parameters with errors in the determination of

* *Note added in proof.* Since this manuscript was written the improvements suggested in this section have been tried and have not been successful. A new numerical technique for correcting observed chromatograms, which eliminates some of the limitations of the Fourier Transform method, has been developed and will be published elsewhere (*18*).

TABLE 8

Results for Experimental Test Samples

Statistic	Run				
	181-185	196-302-1	196-305-1	196-306-1	196-308-1
$10^{-3}\bar{M}_n(\infty)$	133.3	69.0	25.7	38.8	51.5
$10^{-3}\bar{M}_w(\infty)$	364.5	87.8	34.2	51.4	78.3
$P(\infty)$	2.72	1.28	1.33	1.32	1.52
$10^{-3}\bar{M}_n(t)_w$[a]	137.2	74.0	26.8	43.7	56.2
$10^{-3}\bar{M}_w(t)_w$	352.7	91.1	33.8	56.5	85.1
$P(t)_w$	2.57	1.23	1.31	1.29	1.51
$10^{-3}\bar{M}_n(t)_E$[b]	144.0	71.8	26.6	40.0	53.5
$10^{-3}\bar{M}_w(t)_E$	328.4	83.5	32.6	49.2	74.7
$P(t)_E$	2.26	1.27	1.22	1.22	1.40
Raw area (smoothed)[c]	92.57	88.22	85.71	91.42	87.22
Corrected area[d]	94.35	93.81	84.28	104.1	94.43
Raw MEV	28.12	30.24	32.44	31.46	30.65
m_2	3.928	1.192	1.400	1.40	2.11
μ_2 at MEV	0.7311	0.4487	0.3940	0.3840	0.4200
Predicted m_2^*[e]	3.197	0.7435	1.005	1.017	1.680
Corrected m_2^*	3.670	1.045	1.133	1.278	2.090
k_{max} from Eq. (70)	2.76	5.73	4.92	4.89	3.80
Δk	$\pi/100$	$\pi/40$	$\pi/50$	$\pi/50$	$\pi/60$
k_{max} used[f]	2.73	5.65	4.90	4.83	3.76

[a] All the statistics with a subscript w are those calculated from the corrected chromatogram $W(v)$.

[b] All the statistics with a subscripted E are those calculated from Eqs. (47) and (48).

[c] All the statistics preceded by the word "raw" are those calculated from $F(v)$, the normalized observed chromatogram.

[d] All the statistics preceded by the word "corrected" are those calculated from the $W(v)$ obtained from $F(v)$ by the numerical Fourier transformation procedures.

[e] All the statistics preceded by the word "predicted" are those calculated from the relations in Table 2.

[f] k_{max} used refers to the actual largest value of k used to evaluate $F(k)$.

the experimental values of $\bar{M}_n$ and $\bar{M}_w$. It may be better to separate the determination of the instrument spreading parameters from the experimental values of $\bar{M}_n$ and $\bar{M}_w$ because these parameters should be dependent only on the flow behavior of the polymer molecules through the GPC columns. This may be done by assuming that Eqs. (62), (63), and (64) adequately describe the observed chromatogram of a nearly monodisperse standard.

Then μ_2, μ_3, and μ_4 are directly obtained from the moments of the $F(v)$ curve.

$$\mu_2 = m_2 \tag{75}$$

$$\mu_3 = m_3 \tag{76}$$

$$\mu_4 = m_4$$

Plots of μ_2, μ_3, and μ_4 vs MEV would then result. The plot of μ_3 vs MEV would be quite different from that obtained by directly using $\bar{M}_n(t)$ and $\bar{M}_w(t)$ data. This difference would be reflected in the molecular weight calibration curve to be determined by the method described below.

Since $F(v) \approx W(v)$ for each MEV, then the Yau-Malone parameters can be sought such that $\bar{M}_n(t)_w$ and $\bar{M}_w(t)_w$ are fit as closely as possible to the experimentally determined values of $\bar{M}_n(t)$ and $\bar{M}_w(t)$. In this way experimental errors associated with $\bar{M}_n(t)$ and $\bar{M}_w(t)$ would be smeared out over the entire calibration curve.

A major source of difficulty in the numerical Fourier transform method is the determination of the proper value of $k_{\max}$ at which to stop the evaluation of $W(k)$ before the effects of noise in the numerical $F(v)$ data and roundoff errors prevent $|F(k)|$ and thus $|W(k)|$ from smoothly approaching zero. If $F(k)$ can be fit by a function having a generalized form of the type shown in Eq. (65), then $W(k)$ may be expressed by an analytical function of the form similar to Eq. (66), which appears to have better numerical properties in that $|W(k)|$ will be forced to smoothly approach zero. As was shown previously, the Fourier transform method, indeed, does work well on analytically generated data.

Acknowledgments

The authors would like to acknowledge the contributions of Mr. Wilfred J. Renaudette and Mr. James H. Clark for assistance in the experimental GPC work and data reduction calculations, respectively.

List of Symbols*

A, B, C, D	parameters of the Yau-Malone nonlinear molecular weight calibration curve as defined by Eq. (40) and illustrated by Fig. 3
a_j, b_j	intercept and slope parameters of a straight line segment approximating $F(v)$ over jth interval for the Filon Quadrature method

* Symbols and notation found in the text and not defined here have been previously described in (I.).

C_3, C_4	skewness and flatness coefficients of the analytical skewed Gaussian function described by Eq. (62)
DFT	discrete Fourier transform
FFT	fast Fourier transform
$\|F(k)\|_{\min}$	minimum value of $\|F(k)\|$ chosen as the point in k-space to terminate the evaluation of $F(k)$
$F_j(z)$	value of $F(v)$ over jth interval approximated by straight line segment
$F_1(k)$, $F_2(k)$	real and imaginary parts of the Fourier transformation of the observed chromatogram $F(v)$ about v_0 as defined by Eqs. (29), (32), and (33)
H	resolution factor as defined by Tung (*3*) and described by Eq. (72)
(I.)	Paper I of this series described in Ref. *1*
$k_{\max}$	the maximum value of k in k-space out to which $F(k)$ should be evaluated
MEV	mean elution volume
$\bar{M}_n(t)_E$	value of number-average molecular weight obtained from values of μ_2, μ_3, and μ_4 at the MEV used in Eq. (47)
$\bar{M}_n(\infty)_s$, $\bar{M}_n(t)_s$	smoothed infinite resolution and true number-average molecular weights, respectively, by use of the Yau-Malone function, Eq. (40)
$\bar{M}_n(t)_w$	number-average molecular weight calculated from corrected chromatogram, $W(v)$
$\bar{M}_w(t)_E$	value of weight-average molecular weight obtained from values of μ_2, μ_3, and μ_4 at the MEV used in Eq. (48)
$\bar{M}_w(\infty)_s$, $\bar{M}_w(t)_s$	smoothed infinite resolution and true weight-average molecular weights, respectively, obtained by use of the Yau-Malone function, Eq. (40)
$\bar{M}_w(t)_w$	weight-average molecular weight calculated from corrected chromatogram, $W(v)$
m_2^*, m_3^*, m_4^*	second, third, and fourth moments about the mean of the corrected chromatogram, $W(v)$
$P(t)_E$	value of the polydispersity ratio obtained from the values of μ_2, μ_3, and μ_4 at the MEV used in Eqs. (47) and (48)
$P(\infty)_s$, $P(t)_s$	smoothed infinite resolution and true polydispersity ratio, respectively

$P(t)_w$ polydispersity ratio obtained from the corrected chromatogram, $W(v)$

v_0 elution volume at center of the chromatogram about which to transform the range of integration in Eqs. (25) and (26)

v_s specified elution volume at which $(dv/dM)_{v_s}$ is to be evaluated

$\langle v^3 \rangle$ third moment about the origin of the normalized observed chromatogram

$\langle y^3 \rangle$ third moment about the origin of the normalized corrected chromatogram

$W_1(k)$, $W_2(k)$ real and imaginary parts of the Fourier transformation of the corrected chromatogram $W(v)$ about v as defined by Eqs. (29), (35), and (36)

z transformed variable defined by Eq. (29)

Greek Letters

α reduced parameter defined by Eq. (49)

β_1, β_2 reduced parameters of $G(v - y)$ function defined by Eqs. (6) and (7)

μ mean elution volume

ψ reduced parameter of Yau-Malone function defined by Eq. (41)

REFERENCES

1. T. Provder and E. M. Rosen, *Separ. Sci.*, **5**, 437 (1970).
2. W. W. Yau and C. P. Malone, *J. Polym. Sci., Part B*, **5**, 663 (1967).
3. L. H. Tung, *J. Appl. Polym. Sci.*, **13**, 775 (1969).
4. H. T. Davis, *Introduction to Nonlinear Differential and Integral Equations*, U.S. Atomic Energy Commission, Supt. of Documents, Washington, D.C., 1960, pp. 434ff.
5. V. S. Pugachev, *Theory of Random Functions*, Addison-Wesley, New York, 1962. pp. 44ff.
6. H. Freeman, *Introduction to Statistical Inference*, Addison-Wesley, New York, 1963, Chapter 18.
7. E. Grushka, M. N. Myers, P. D. Schettler, and J. C. Giddings, *Anal. Chem.*, **41**, 889 (1969).
8. D. E. Barton and K. E. Dennis, *Biometrika*, **39**, 425 (1952).
9. G-AE Subcommittee on Measurement Concepts, *IEEE Trans. Audio Electroacoustics*, **AU-15(2)**, 45 (1967).
10. G. D. Bergland, *IEEE Spectrum*, **41**, (July 1969).
11. S. M. Chase and L. D. Fosdick, *Commun. Ass. Comput. Mach.*, **12**, 457 (1969).

12. A. Papoulis, *The Fourier Integral and Its Applications,* McGraw-Hill, New York, 1962, pp. 20f.
13. P. W. Murrill, R. W. Pike, and C. L. Smith, *Chem. Eng.,* **76,** 105 (February 1969).
14. K. J. Bombaugh, W. A. Dark, and R. F. Levangie, *Separ. Sci.,* **3,** 375 (1968).
15. D. W. Marquardt, *J. Soc. Ind. Appl. Math.,* **2,** 431 (1963).
16. E. J. Henley and E. M. Rosen, *Material and Energy Balance Computations,* Wiley, New York, 1969, pp. 547f and 560-566.
17. H. E. Pickett, M. J. R. Cantow, and J. F. Johnson, *J. Appl. Polym. Sci.,* **10,** 917 (1966).
18. E. M. Rosen and T. Provder, Paper to be presented at the Ninth International GPC Seminar, Miami Beach, Florida, October, 1970.

Received by editor February 23, 1970